Research article

LUMINESCENCE
The Journal of Biological and Chemical Luminescence

Received: 28 September 2015, Revised: 21 January 2016, Accepted: 25 January 2016 Published online in Wiley Online Library

(wileyonlinelibrary.com) DOI 10.1002/bio.3117

Reaction-based probe for hydrogen sulfite: dual-channel and good ratiometric response

Xiaohong Cheng,[a]* Ping He,[b] Zhicheng Zhong[a] and Guijie Liang[a]

ABSTRACT: We designed and synthesized a new series of intramolecular charge transfer (ICT) molecules (compounds T1, T2 and T3) by attaching various electron-donating thiophene groups to the triphenylamine backbone with aldehyde group as the electron acceptor. Based on the nucleophilic addition reaction between hydrogen sulfite and aldehyde, all compounds could act as ratiometric optical probe for hydrogen sulfite and displayed efficient chromogenic and fluorogenic signaling. Upon the addition of hydrogen sulfite anions, probe T3 displayed apparent fluorescent color changes from yellowish-green to blue, with a large emission wavelength shift ($\Delta\lambda$ = 120 nm). T3 responded to hydrogen sulfite with high sensitivity and the detection limit was determined to be as low as 0.9 μM. At the same time, apparent changes in UV–vis spectra could also be observed. By virtue of the special nucleophilic addition reaction with aldehyde, T3 displayed high selectivity over other anions. Copyright © 2016 John Wiley & Sons, Ltd.

Additional supporting information may be found in the online version of this article at the publisher's web site.

Keywords: reaction-based probe; fluorescence; colorimetric; hydrogen sulfite; intramolecular charge transfer

Introduction

In recent decades, efficient detection for anions has attracted considerable attention because of their importance in a large number of biological processes (1–6). Among these anions, hydrogen sulfite has been widely used as a preservative for foods, beverages and pharmaceutical products (fish, potatoes, wine, etc.). However, bisulfite has been associated with allergic reactions and food intolerance symptoms such as difficulty in breathing, wheezing, hives, and gastrointestinal distress (7–9). The acceptable daily intake (ADI) of sulphite (expressed as SO_2) is 0.7 mg/kg set by the European Parliament and Council Directives (10). Therefore, the development of a sensitive and selective method for the determination of hydrogen sulfite is of great importance for food safety and quality control, clinical and environmental applications.

In the field of chemosensors, fluorescent sensors possess innate advantages because of their high sensitivity, specificity, simplicity of implementation, and fast response times, offering application methods not only for *in vitro* assays but also for *in vivo* imaging studies (11,12). Meanwhile, colorimetric sensors are especially promising because the color change can easily be observed by the naked eye, thus requiring less labor and no equipment (13–18). Therefore, it is reasonable that the dual-channel chemosensors, which have both fluorescent and colorimetric responses toward the analytes, can integrate the above two advantages. In addition, a ratiometric optical method can enable the measurement of absorption/emission intensities at two different wavelengths, providing a built-in correction for environmental effects and also increasing the dynamic range of measurement (19–24). However, the dual-channel probes for both fluorogenic and chromogenic detection of hydrogen sulfite are still very scarce so far, especially the ratiometric ones (25–29).

As an emerging approach, the reaction-based probes, which involve the use of special chemical reactions induced by target analytes, provide us with versatile means for investigating a wide range of analytes with superior selectivity (30–34). In basic organic chemistry, aldehyde is known to react with hydrogen sulfite to form an aldehyde–hydrogen sulfite adduct (35). Considering that the conversion of the aldehyde into the hydrogen sulfite adduct would bring about a change in the electron acceptor strength and the concomitant intramolecular charge transfer (ICT) efficiency, it is feasible to design chemosensors based on this process, for the detection of hydrogen sulfite anion (Scheme 1). Meanwhile, thiophenes are ideal building blocks to provide the basis for the synthesis of conjugated π-systems (36). With these considerations in mind, here, we speculated whether dual-channel and good ratiometric response probes for hydrogen sulfite could be designed by the modification of ICT efficiency of the thiophene-containing molecules in and without the presence of hydrogen sulfite.

To this end, a new series of ICT molecules (compounds T1, T2 and T3, Scheme 2) was synthesized by attaching various electron-donating thiophene groups to a triphenylamine (TPA) backbone with the aldehyde group as the fixed electron acceptor. The electron-rich TPA-thiophene moiety was selected to act as both a fluorescent dye and electron donor in the ICT process, which was the key to the success of this strategy (37). The aldehyde group was chosen to function as an electron acceptor in

* Correspondence to: Xiaohong Cheng, Hubei Key Laboratory of Low Dimensional Optoelectronic Materials and Devices, Hubei University of Arts and Science, Xiangyang 441053, Hubei Province, People's Republic of China. E-mail: chengxiaohong0807@126.com

[a] Hubei Key Laboratory of Low Dimensional Optoelectronic Materials and Devices, Hubei University of Arts and Science, Xiangyang 441053 Hubei Province, People's Republic of China

[b] College of Chemical Engineering and Food Science, Hubei University of Arts and Science, Xiangyang 441053 Hubei ProvincePeople's Republic of China

Abbreviations: ADI, acceptable daily intake; ICT, intramolecular charge transfer

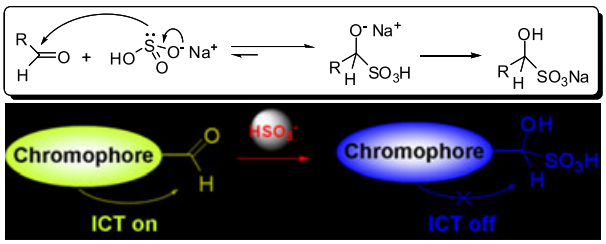

Scheme 1. The process of nucleophilic addition reaction between aldehyde and $NaHSO_3$ and the resulting changed ICT efficiencies and optical properties.

the ICT process on the one hand, and to act as a putative hydrogen sulfite-dependent reactive subunit on the other hand. Based on the triphenylamine backbone, the thiophene and ethylenedioxythiophene moieties were introduced to enhance the efficiency of the donor to benefit the delocalization of the whole chromophore, respectively, in compounds T1 and T3. Then, we linked bithiophene moieties to the backbone to extend the length of the π conjugation to prepare compound T2. As demonstrated in Scheme 2, the aldehyde T3 emitted yellowish-green fluorescence with the quantum yield of ~0.30. After the reaction with hydrogen sulfite anions, the resulting aldehyde–hydrogen sulfite adduct displayed strong blue fluorescence with the increasing quantum yield of about 0.51. Correspondingly, the color of its solution changed from yellow to colorless. This indicated that after the addition reaction of aldehyde, the electronic property of the resultant hydrogen sulfite adduct changed, leading to the different fluorescent behavior due to the different ICT efficiency. Herein, we would like to describe the synthesis and the spectroscopic evaluation of the dual-channel chemosensors in detail.

Experimental

Materials and instrumentations

Double-distilled water was used in all experiments. Inorganic salts including $NaHSO_3$, $NaOAc{\cdot}3H_2O$, $NaNO_2$, $NaNO_3$, NaF, Na_2CO_3, Na_2SO_4, Na_3PO_4, NaCl, $NaIO_3$, $KClO_3$, KBr, KSCN, KI, $NaHSO_4$, $Na_2S{\cdot}9H_2O$ and $Na_2S_2O_3{\cdot}5H_2O$ were purchased from Shanghai Chemical Reagent Co. (Shanghai, China). All solvents and other reagents were of analytical grade and purchased from the Sigma-Aldrich Chemical Company. *N,N*-Dimethylformamide (DMF) was dried over and distilled from CaH_2 under an atmosphere of dry nitrogen. Tetrahydrofuran (THF) was dried over and distilled from a K–Na alloy under an atmosphere of dry nitrogen. All other reagents were used as purchased. Compounds 1–4 were synthesized according to the literature procedures (38).

The ^1H and ^{13}C NMR spectra were measured on Varian Mercury300 and Bruker Avance III400 spectrometer. The ESI (???) mass spectra were measured on a Finnigan LCQ advantage mass spectrometer (RT: 4.97–5.38; AV: 26; NL: 8.42E6). The pH values were determined using a DELTA 320 PH dollar meter. Photoluminescence spectra were performed on a Hitachi F-4500 fluorescence spectrophotometer. UV–vis spectra were obtained using a Shimadzu UV-2550 spectrometer. Fourier transform infrared (FTIR) spectra were recorded on a PerkinElmer-2 spectrometer in the region of 3000–400 cm^{-1} on NaCl pellets.

General procedure for synthesis of compounds T1, T2 and T3

Compound 5, or 6, or 7 (1 equiv.) was dissolved in $ClCH_2CH_2Cl$, then $POCl_3$ (2.7 equiv.) in DMF was added dropwise to the mixture at 0°C. After the temperature rose to room temperature, the reaction was heated to 45°C. After cooling, the mixture was poured in an ice bath with stirring and later neutralized with sodium carbonate. The mixture was then filtered, and the crude product was purified by column chromatography on silica gel to produce the resulting powder.

Synthesis of compound T1. Compound 5 (0.51 g, 1.0 mmol), DMF (0.5 mL, 6.5 mmol), $POCl_3$ (0.25 mL, 2.7 mmol), $ClCH_2CH_2Cl$ (25 mL). Using petroleum ether/$CHCl_3$ (1:1, *v*/v) as eluent to obtain T1 as an orange powder (0.30 g, 56%). ^1H NMR (400 MHz, $CDCl_3$, ppm): 9.84 (s, 1H, −CHO), 7.65 (s, 1H, Ar-H), 7.35–7.38 (m, 6H, Ar-H), 7.09–7.12 (m, 3H, Ar-H), 7.00–7.03 (d, 2H, −CH = CH–), 6.95–6.98 (m, 4H, Ar-H). ^{13}C NMR ($CDCl_3$) *δ:* 182.5, 152. 7, 146.0, 141.3, 137.2, 130.8, 123.6, 119.5, 116.2. MS (???) (ESI), m/z $[M + H]^+$: 540.2, calcd, 539.9.

Synthesis of compound T2. Compound 6 (0.59 g, 1.0 mmol), DMF (1 mL, 13.0 mmol), $POCl_3$ (0.37 mL, 4.04 mmol), $ClCH_2CH_2Cl$ (50 mL). Using petroleum ether/$CHCl_3$ (1:2, *v*/v) as eluent to obtain T2 as a yellow powder (0.36 g, 58%). ^1H NMR (300 MHz, $CDCl_3$, ppm): 9.84 (s, 1H, −CHO), 7.70–7.72 (d, 2H, *J* = 6.0 Hz, Ar-H), 7.61–7.64 (d, 2H, *J* = 9.0 Hz, Ar-H), 7.52–7.54 (m, 4H, Ar-H), 7.04–7.07 (d, 2H, *J* = 9.0 Hz, −CH = CH–), 6.88–6.90 (d, 4H, *J* = 6.0 Hz, Ar-H), 6.79–6.82 (d, 4H, *J* = 9.0 Hz, Ar-H). ^{13}C NMR ($CDCl_3$) *δ:* 182.7, 146.3, 137.7, 132.7, 129.3, 127.8, 127.3, 126.1, 124.0, 120.2, 116.3. MS (ESI), m/z $[M + H]^+$: 621.8, calcd, 621.9.

Synthesis of compound T3. Compound 7 (1.14 g, 2.0 mmol), DMF (1 mL, 13.0 mmol), $POCl_3$ (0.5 mL, 5.35 mmol), $ClCH_2CH_2Cl$ (50 mL). Using petroleum ether/$CHCl_3$ (1:1, *v*/v) as eluent to obtain **1** as an orange powder (1.00 g, 83.7%). ^1H NMR (300 MHz, $CDCl_3$, ppm):

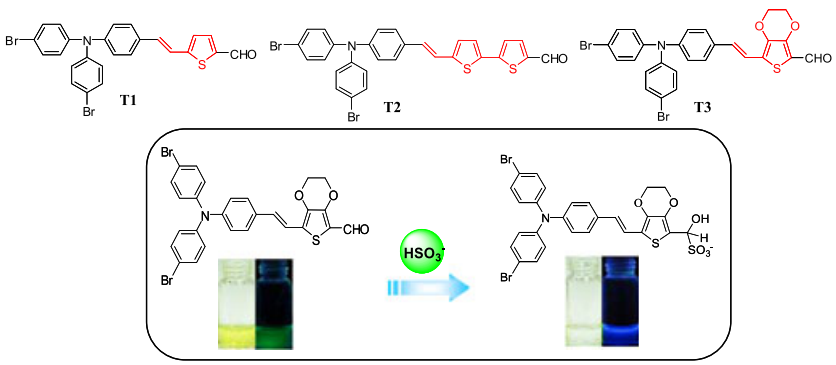

Scheme 2. Structures of compounds T1, T2 and T3 and the sensing process of T3 toward HSO_3^-.

LUMINESCENCE
The Journal of Biological and Chemical Luminescence

9.87 (s, 1H, −CHO), 7.56–7.58 (d, 2H, J = 6.0 Hz, Ar-H), 7.47–7.50 (m, 4H, Ar-H), 7.18 (s, 2H, −CH = CH–), 7.03–7.06 (m, 6H, Ar-H), 4.45–4.50 (m, 4H, $-CH_2-CH_2-$). ^{13}C NMR ($CDCl_3$) δ: 179.5, 148.9, 147.3, 146.2, 138.7, 132.7, 131.4, 131.0, 128.6, 128.2, 126.2, 123.7, 116.5, 116.3, 115.5, 65.6, 64.8. MS (ESI), m/z $[M + H]^+$: 597.9, calcd, 598.0.

Preparation of solutions of anions

One millimole of each inorganic salt ($NaHSO_3$, $NaOAc{\cdot}3H_2O$, $NaNO_2$, $NaNO_3$, NaF, Na_2CO_3, Na_2SO_4, Na_3PO_4, NaCl, $NaIO_3$, $KClO_3$, KBr, KSCN, KI, $NaHSO_4$, $Na_2S{\cdot}9H_2O$ and $Na_2S_2O_3{\cdot}5H_2O$) was dissolved in distilled water (10 mL) to afford 1×10^{-1} mol/L aqueous solution. The stock solutions were diluted to desired concentrations with water when needed.

Fluorescence titration of T3 with HSO_3^-

A solution of T3 (10 μM) was prepared in THF–H_2O solution (8:2, *v*/v). A 200 mM NaH_2PO_4 citric buffer solution (pH 5.0) was employed. Then 3.0 mL of the solution of T3 was placed in a quartz cell (10.0 mm width) and the fluorescence spectrum was recorded. The $NaHSO_3$ solution was introduced in portions (the effect on the total volume of solution induced by the addition of hydrogen sulfite was negligible) and fluorescence intensity changes were recorded at room temperature each time (excitation wavelength: 400 nm; excitation slit: 5.0 nm; emission slit: 2.5 nm; fluorescence emission spectra were uncorrected).

Fluorescence intensity changes of T3 with other anions

A solution of T3 (10 μM) was prepared in THF–H_2O solution (8:2, *v*/v, 200 mM NaH_2PO_4 citric buffer, pH 5.0). Then 3.0 mL of the solution of T3 was placed in a quartz cell (10.0 mm width) and the fluorescence spectrum was recorded. Different anion solutions were introduced and the changes of the fluorescence intensity were recorded at room temperature each time (excitation wavelength: 400 nm; excitation slit: 5.0 nm; emission slit: 2.5 nm; fluorescence emission spectra were uncorrected).

Quantum yield changes of T3 with HSO_3^-

Quantum yield was determined according to the equation as follows:

$$\Phi_{F(sample)} = \left(\frac{A_{standard}}{A_{sample}}\right)\left(\frac{F_{sample}}{F_{standard}}\right)\Phi_{F(standard)}$$

Φ_F was the fluorescence quantum yield, A was the absorbance, F was the area under the corrected emission curve. Here, fluorescein was used as the standard; the quantum yield of fluorescein in 0.1 M NaOH was 0.90 (39).

UV–vis absorption changes of T3 by HSO_3^-

A solution of T3 (20 μM) was prepared in THF–H_2O solution (8:2, *v*/v, 200 mM NaH_2PO_4 citric buffer, pH 5.0). Then 3.0 mL of the solution of T3 was placed in a quartz cell (10.0 mm width) and the absorption spectrum was recorded. The $NaHSO_3$ aqueous solution was introduced in portions (the effect on the total volume of solution induced by the addition of hydrogen sulfite was negligible) and the absorption spectra were recorded at room temperature each time (slit width: 2.0 nm).

Results and discussion

Synthesis and structural characterization

The general synthetic procedure is presented in Scheme 3. The Wittig reaction of the obtained diethyl ((4-(diphenylamino)benzyl) triphenyl)-phosphonate (1) with 2-formyl-thiophene and derivatives (2–4) gave the corresponding triphenylamine-vinyl thiophene (5–7). The followed Vilsmeier reaction of 5, 6 or 7 yielded the corresponding aldehyde T1, T2 or T3. All compounds exhibited good solubility in common organic solvents, such as $CHCl_3$, acetone, DMF, DMSO, CH_3CN, and THF. Their structures were well characterized by ^1H, ^{13}C NMR, and ESI-MS, and all gave satisfactory spectral data (see Supplementary Material Figs S1–S9).

The UV–vis absorption and fluorescent emission spectra for the ICT molecules are shown in Fig. S10 and summarized in Table 1. Both the different absorption and emission behaviors between the aldehydes and the precursors demonstrated the changes of the electronic properties, leading to different ICT efficiency.

Optimization of experimental conditions

As shown in Fig. 1, all compounds displayed two well separated emission peaks before and after the addition of hydrogen sulfite,

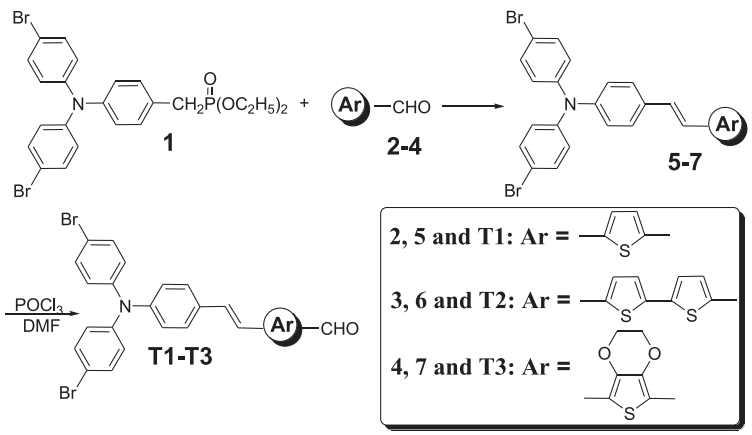

Scheme 3. General procedures for the synthesis of T1, T2 and T3.

Table 1. Optical data of sensor molecules

	λ_{abs} (nm)	λ_{em} (nm)		λ_{abs} (nm)	λ_{em} (nm)		λ_{abs} (nm)	λ_{em} (nm)
5	310	448	6	310	497	7	383	440
T1	353	535	T2	354	570	T3	420	560

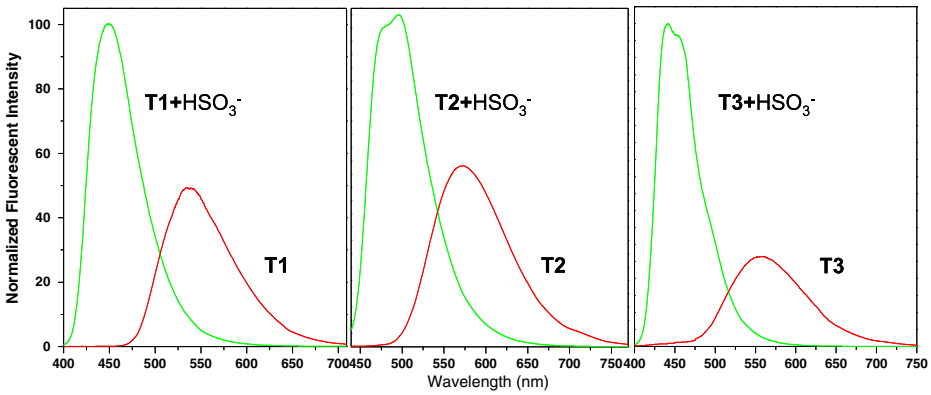

Figure 1. The fluorescent spectra of probe and probe + HSO_3^-.

thus potentially all of them could act as the ratiometric fluorescent probe for HSO_3^-. However, with the addition of excess hydrogen sulfite, compound T3 exhibited the largest emission wavelength shift (from 560 to 440 nm, $\Delta\lambda$ = 120 nm) and largest enhancement in the ratiometric value (995-fold) compared with that of the counterpart T1 (from 535 to 450 nm, $\Delta\lambda$ = 85 nm, 500-fold) and T2 (from 570 to 495 nm, $\Delta\lambda$ = 75 nm, 415-fold). As mentioned above, the ultimate goal of this research was to develop a reactive probe for hydrogen sulfite with a good ratiometric optical response. Therefore, we chose compound T3 as the representative of the ICT-type molecules in the following titration experiment.

First, the effect of pH values on the reaction was investigated, with the results summarized in Fig. S11. The pH value of 5.0 (200 mM Na_2HPO_4–citric acid buffer) was chosen, in order to ensure the analyte anion as the chemically reactive hydrogen sulfite but not sulfite or sulfur dioxide. In the titration experiment, the mixture system with THF/H_2O = 8:2 was chosen as the reaction media. As shown in Fig. S12, after the addition of excess hydrogen sulfite, the largest ratiometric value of I_{440}/I_{560} could be achieved with 80% of THF, which was beneficial to the design of a ratiometric fluorescence probe. The possible reason was that there were solubility differences between the probe and the addition product and different existing forms of them would affect the fluorescent measurement. Meanwhile, considering that the optical signal changes relied on the chemical reaction between compound T3 and HSO_3^-, and then the reaction rate might affect the experimental results, we investigated the influence of the reaction time on the probing results, and the obtained results were demonstrated in Fig. S13. At lower concentrations of HSO_3^- (1×10^{-5}, 2×10^{-5} and 3×10^{-5} M), there were gradual changes in the emission intensity from 0 to 8 minutes; however, after 8 min, the changes became smaller than before. With the increasing of the concentrations of HSO_3^-, such as 5×10^{-5}, 7×10^{-5} and 9×10^{-5} M, a plateau of intensity could be achieved after 10 min and the changes became slight from 10–14 min. Thus, in the titration experiment, we measured the optical intensity changes of the T3 solutions 10 min later after all the species were added.

Sensing properties

The sensing behavior of T3 toward hydrogen sulfite was investigated carefully under the optimized conditions. As shown in Fig. 2, increasing the concentration of hydrogen sulfite, the maximum emission wavelength shifted from 560 to 440 nm with a well defined isoemissive point at 515 nm. Actually, even at the concentration of hydrogen sulfite as low as 3 μM, apparent spectra changes could be observed with respect to the blank solution. It was noteworthy that the difference in the two emission wavelengths was very large (emission shift: $\Delta\lambda$ = 120 nm), which not only contributed to the accurate measurement of the intensities of the two emission peaks, but also resulted in a huge ratiometric value. Actually, in the presence of 90 μM of hydrogen sulfite, a *c.* 1000-fold enhancement in the ratiometric value of I_{440}/I_{560} (from 0.04 to 39.83) was achieved with respect to the hydrogen sulfite-free solution.

To see the sensing process more visually, we compared the intensities at the two different wavelengths with the results

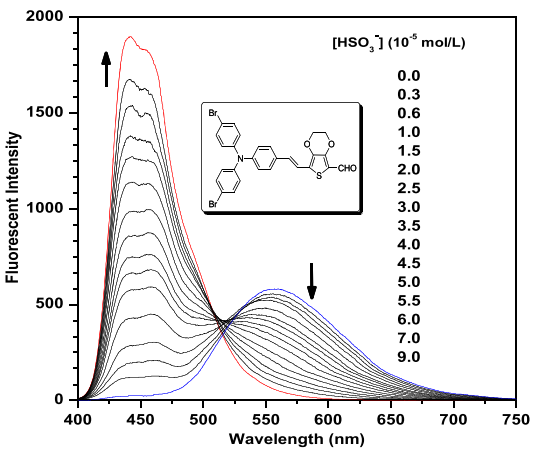

Figure 2. Fluorescent emission spectra of T3 (10 μM, in THF/H_2O = 8/2, pH 5.0) in the presence of different concentrations of HSO_3^- excited at 400 nm.

LUMINESCENCE
The Journal of Biological and Chemical Luminescence

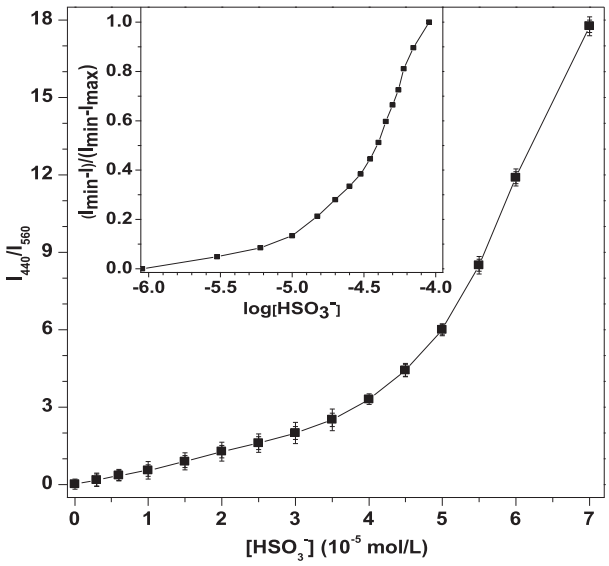

Figure 3. Ratiometric calibration curve I_{440}/I_{560} of T3 (10 μM, in THF/H_2O = 8/2, pH 5.0) as a function of the concentration of HSO_3^- (λ_{ex} = 400 nm). The error bars represent the standard deviation of three measurements. Inset: the intensity at 440 nm changes of T3 as a function of the concentration of HSO_3^-.

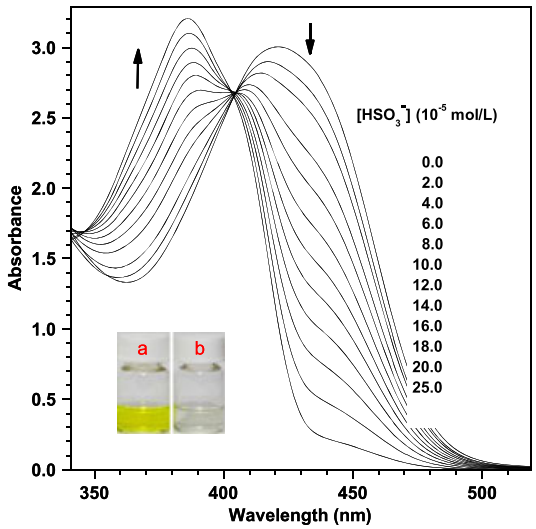

Figure 4. UV–vis absorption spectra of T3 (20 μM, in THF/H_2O = 8/2, pH 5.0) in the presence of different concentrations of HSO_3^-. Inset: photograph of the solution of T3 (a); and T3 + HSO_3^- (b).

summarized in Fig. 3. The error bars for three repeated measurements showing the good reproducibility of this sensing method. Furthermore, the detection limit (40) for the analysis of hydrogen sulfite was estimated from the plot of fluorescence intensity changes at 440 nm versus concentration of added HSO_3^- and was found to be as low as 0.9×10^{-6} M as demonstrated in the inset of Fig. 3. Taking advantage of the same approach, Yang *et al.* prepared a rhodamine-based fluorescent probe toward hydrogen sulfite and the detection limit was reported as 0.89×10^{-6} M (26). In addition, Guo *et al.* designed a series of coumarin-based fluorescent probes for selective detection of hydrogen sulfite anions with the detection limit as 0.37×10^{-6} M (27). Recently, Guo *et al.* reported a 1,8-naphthalimide fluorophore based probe for HSO_3^- and the detection limit was determined to be 0.1×10^{-6} M (28). Compared with these reported works, it was clear that the performance of T3 was among the best results of the hydrogen sulfite chemosensors with the same sensing approach.

In addition to the changed fluorescent behavior caused by the tuned ICT efficiency of T3 in the presence of hydrogen sulfite, the color change was another apparent property. As shown in Fig. 4, with the increasing concentrations of hydrogen sulfite, the maximum absorption wavelength gradually shifted from 420 nm to 385 nm, which was responsible for the color change (from yellow to colorless) and perceptible to the naked eye (inset in Fig. 4). Thus, these results indicated that after the addition reaction of aldehyde, the electronic property of the resultant hydrogen sulfite adduct changed, resulting in the different optical behavior due to the different ICT efficiency.

As is well known, the addition reaction of aldehyde with hydrogen sulfite is chemically reversible. The typical approaches for regenerating the aldehydes from the addition bisulfite adducts found in the literature involved treating the bisulfite adducts with either acid or base. Herein, we investigated the effect of pH on the emission intensity at 440 nm as shown in Fig. S14. Upon adjusting the pH to 9.0, 10.0 and further to 11.0, the solution of T3 displayed apparent fluorescent color changes from blue to yellowish-green and the color changes from colorless to yellow, indicating that the equilibrium of the reaction in Scheme 1 moved toward the left. The above experiment results proved that the proposed recognition reaction was reversible.

To evaluate the specific nature of T3 toward hydrogen sulfite, the influence of other anions were investigated. As shown in Fig. 5, for all other anions including AcO^-, NO_2^-, NO_3^-, F^-, CO_3^{2-}, SO_4^{2-}, PO_4^{3-}, Cl^-, IO_3^-, ClO_3^-, Br^-, SCN^-, I^-, HSO_4^-, S^{2-} and $S_2O_3^{2-}$, there were nearly no changes in the fluorescence spectra observed and the different sensing behavior could be easily seen by the naked eye under a normal ultraviolet (UV) lamp (as displayed in the inset fluorescence photograph in Fig. 5). Moreover, we measured the response of T3 to hydrogen sulfite in the presence of other competitive anions. As shown in Fig. 6, the presence of other background anions did not show any obvious disturbance with the signal response induced by hydrogen sulfite. As reported, aldehyde could also serve as a reactive subunit toward other biological nucleophiles such as cysteine, homocysteine and glutathione (41–43). However, the nucleophilic addition reaction promoted by biological nucleophiles needed much longer time

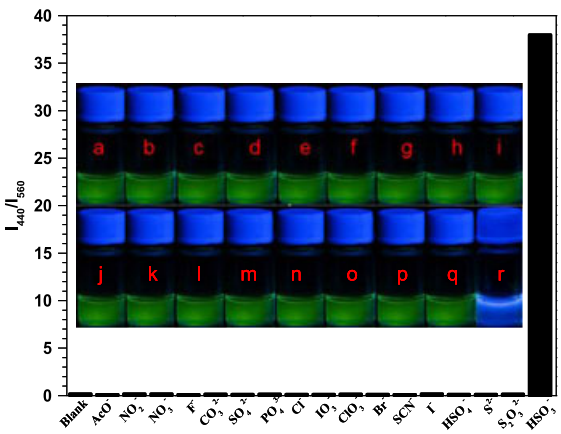

Figure 5. Ratiometric emission of T3 (10 μM, in THF/H_2O = 8/2, pH 5.0, λ_{ex} = 400 nm) in the presence of different anions (HSO_3^-, 90 μM; others, 200 μM). Inset: fluorescent photograph of T3 to various anions. (a) T3; (b–r) T3 + AcO^-, NO_2^-, NO_3^-, F^-, CO_3^{2-}, SO_4^{2-}, PO_4^{3-}, Cl^-, IO_3^-, ClO_3^-, Br^-, SCN^-, I^-, HSO_4^-, S^{2-}, $S_2O_3^{2-}$, HSO_3^-.

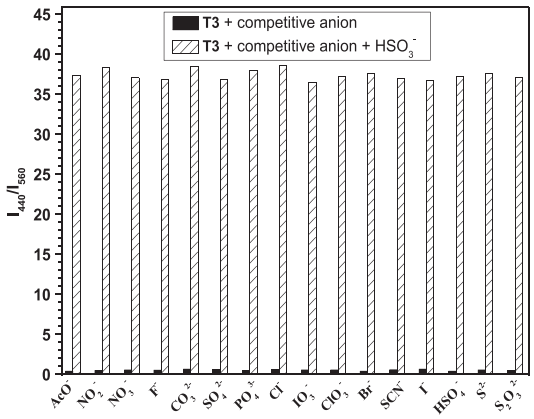

Figure 6. Ratiometric emission of T3 (10 μM, in THF/H_2O = 8/2, pH 5.0, λ_{ex} = 400 nm) to HSO_3^- (90 μM) in the presence of other competitive ions (200 μM).

to complete due to their steric hindrance effect. The above results indicated that our probe had selective response toward hydrogen sulfite over other anions. It was noteworthy that under the optimized sensing conditions (pH = 5.0), these competitive ions might not be in the forms listed above, for instance, a portion of the acetate species would be in the neutral form (acetic acid) at pH 5.0. Here, to simplify the presentation, the anions were described in their added forms as in the other reported works.

To explore the sensing mechanism of T3 to hydrogen sulfite, the reaction mixture of T3 with $NaHSO_3$ was characterized by ESI-MS firstly. As shown in Fig. 7, the ESI-MS spectrum of T3 revealed a main peak at 597.9 nm before the addition of hydrogen sulfite, corresponding to the species $[T3 + H]^+$ (m/z_{caled} = 598.0). After the addition of excess hydrogen sulfite, a relatively weak peak at about 677.0 appeared coinciding exactly with that for the adduct species $[T3 + HSO_3^- - H]^-$ (m/z_{caled} = 676.9). Meanwhile, the infra-red (IR) spectra of T3 before and after the addition of hydrogen sulfite anions could give some information on this transformation. As shown in Fig. 8, a typical absorption peak at about 1655 cm^{-1} appeared in the IR spectrum of T3 in good accordance with aldehyde groups. But after the addition of HSO_3^- ions, no absorption peak centered at about 1655 cm^{-1} was observed in the IR spectrum as the result of the addition reaction between T3 and HSO_3^- anions. Furthermore, compound T1 was treated with 20 equiv. $NaHSO_3$, and the reaction product was characterized by ^1H NMR spectrometry. The partial ^1H NMR spectra of T1 and the hydrogen sulfite adduct were shown in Fig. S15. The resonance signal corresponding to the aldehyde proton (H_a) at 9.84 ppm shifted to 4.65 ppm (H_b), conforming the formation of aldehyde–hydrogen sulfite adduct. The above experimental data indicated that the sensing process most likely followed the proposed mechanism as shown in Scheme 1.

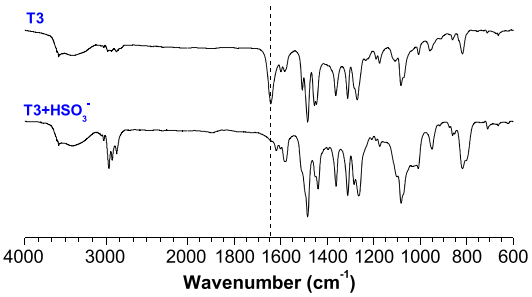

Figure 8. IR spectra of T3 and the product of the reaction between T3 and HSO_3^-.

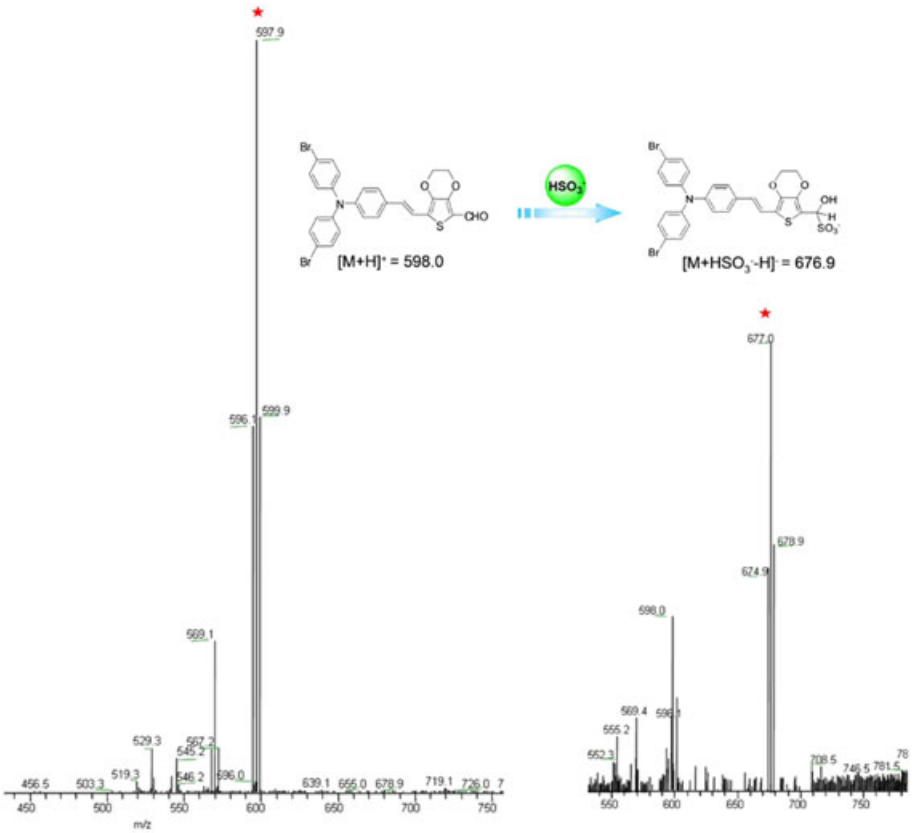

Figure 7. ESI-MS spectra of T3 (left) and the product of the reaction between T3 and HSO_3^- (right).

LUMINESCENCE
The Journal of Biological and Chemical Luminescence

Conclusion

In conclusion, dual-channel probes toward hydrogen sulfite were constructed based on the special nucleophilicity of hydrogen sulfite and the TPA-thiophene chromophore. Upon the addition of hydrogen sulfite anions, probe T3 displayed apparent fluorescent color changes from yellowish-green to blue, with a large emission wavelength shift (emission shift: $\Delta\lambda$ = 120 nm). T3 gave response to hydrogen sulfite with high sensitivity, and the detection limit was determined to be as low as 0.9 μM. At the same time, apparent changes on the UV–vis spectra could also be observed. By virtue of the special nucleophilic addition reaction with aldehyde, T3 displayed high selectivity over other anions. Further study on the design of dual-channel probes for toxic anions with better performance is still in progress in our laboratory.

Acknowledgements

This work was financially supported by the National Natural Science Foundation of China (No. 21502047 and No. 21302047) and the Science and Technology Research Project of Department of Education of Hubei Province (B2015147).

References

1. Rostami A, Taylor MS. Polymers for anion recognition and sensing. Macromol Rapid Commun 2012;33:21–34.
2. Martínez-Máñez R, Sancenón F. Chemodosimeters and 3D inorganic functionalised hosts for the fluoro-chromogenic sensing of anions. Coord Chem Rev 2006;250:3081–93.
3. Kim SK, Kim HN, Zhu X, Lee HN, Soh JH, Swamy KMK, Yoon J. Recent development of anion selective fluorescent chemosensors. Supramol Chem 2007;19:221–7.
4. Kobayashi H, Ogawa M, Alford R, Choyke PL, Urano Y. New strategies for fluorescent probe design in medical diagnostic imaging. Chem Rev 2010;110:2620–40.
5. Gale PA, Garcia-Garrido SE, Garric J. Anion receptors based on organic frameworks: highlights from 2005 and 2006. Chem Soc Rev 2008;37:151–90.
6. Suksai C, Tuntulani T. Chromogenic anion sensors. Chem Soc Rev 2003;32:192–202.
7. McFeeters RF. Use and removal of sulfite by conversion to sulfate in the preservation of salt-free cucumbers. J Food Protect 1998;61:885–90.
8. Yang X, Guo X, Zhao Y. Novel spectrofluorimetric method for the determination of sulfite with rhodamine B hydrazide in a micellar medium. Anal Chim Acta 2002;456:121–8.
9. Fazio T, Warner CR. A review of sulphites in foods: analytical methodology and reported findings. Food Addit Contam 1990;7:433–54.
10. Claudia RC, Francisco JC. Application of flow injection analysis for determination sulphites in food and beverages: a review. Food Chem 2009;112:487–93.
11. Dickerson TJ, Reed NN, LaClair JJ, Janda KD. A precipitator for the detection of thiophilic metals in aqua. J Am Chem Soc 2004;126:16582–6.
12. Yoon S, Albers AE, Wong AP, Chang CJ. Screening mercury levels in fish with a selective fluorescent chemosensor. J Am Chem Soc 2005;127:16030–1.
13. Palomares E, Vilar R, Durrant JR. Heterogeneous colorimetric sensor for mercuric salts. Chem Commun 2004;40:362–3.
14. Sancenón F, Martínez-Máñez R, Soto J. 1,3,5-Triarylpent-2-en-1,5-diones for the colorimetric sensing of the mercuric cation. Chem Commun 2001;37:2262–3.
15. Huang J, Wen W, Sun Y, Chou P, Fang J. Two-stage sensing property via a conjugated donor-acceptor-donor constitution: application to the visual detection of mercuric ion. J Org Chem 2005;70:5827–32.
16. Tatay S, Gavina P, Coronado E, Palomares E. Optical mercury sensing using a benzothiazolium hemicyanine dye. Org Lett 2006;8:3857–60.
17. Wiskur SL, AitHaddou H, Lavigne JJV, Anslyn E. Teaching old indicators new tricks. Acc Chem Res 2001;34:963–72.
18. Brümmer O, Clair JJL, Janda KD. A colorimetric ligand for mercuric ion. Org Lett 1999;1:415–8.
19. Srikun D, Miller EW, Domaille DW, Chang CJ. Application of flow injection analysis for determination sulphites in food and beverages: a review. J Am Chem Soc 2008;130:4596–7.
20. Komatsu K, Urano Y, Kojima H, Nagano T. Development of an iminocoumarin-based zinc sensor suitable for ratiometric fluorescence imaging of neuronal zinc. J Am Chem Soc 2007;129:13447–54.
21. Tremblay MS, Halim M, Sames D. Cocktails of Tb^{3+} and Eu^{3+} complexes: a general platform for the design of ratiometric optical probes. J Am Chem Soc 2007;129:7570–7.
22. Deo S, Godwin HA. Ratiometric fluorescent sensor for Pb^{2+}. J Am Chem Soc 2000;122:174–5.
23. Mello JV, Finney NS. Dual-signaling fluorescent chemosensors based on conformational restriction and induced charge transfer. Angew Chem Int Ed 2001;40:1536–8.
24. Tsien RY, Harootunian AT. Practical design criteria for a dynamic ratio imaging system. Cell Calcium 1990;11:93–109.
25. Mohr GJ. A chromoreactant for the selective detection of HSO_3^- based on the reversible bisulfite addition reaction in polymer membranes. Chem Commun 2002;38:2646–7.
26. Yang X, Zhao M, Wang G. A rhodamine-based fluorescent probe selective for bisulfite anion in aqueous ethanol media. Sensors Actuators B Chem 2011;152:8–13.
27. Chen K, Guo Y, Lu Z, Yang B, Shi Z. Novel coumarin-based fluorescent probe for selective detection of bisulfite anion in water. Chin J Chem 2010;28:55–60.
28. Sun Y, Wang P, Liu J, Zhang J, Guo W. A fluorescent turn-on probe for bisulfite based on hydrogen bond-inhibited C = N isomerization mechanism. Analyst 2012;137:3430–3.
29. Wang G, Qi H, Yang X. A ratiometric fluorescent probe for bisulphate anion, employing intramolecular charge transfer. Luminescence 2013;28:97–101.
30. Jun ME, Roy B, Ahn KH. "Turn-on" fluorescent sensing with "reactive" probes. Chem Commun 2011;47:7583–601.
31. Du J, Hu M, Fan J, Peng X. Fluorescent chemodosimeters using "mild" chemical events for the detection of small anions and cations in biological and environmental media. Chem Soc Rev 2012;41:4511–35.
32. Que EL, Domaille DW, Chang CJ. Metals in neurobiology: probing their chemistry and biology with molecular imaging. Chem Rev 2008;108:1517–49.
33. Kikuchi K Design, synthesis and biological application of chemical probes for bio-imaging. Chem Soc Rev 2010;39:2048–53.
34. Qian X, Xiao Y, Xu Y, Guo X, Qian J, Zhu W. "Alive" dyes as fluorescent sensors: fluorophore, mechanism, receptor and images in living cells. Chem Commun 2010;46:6418–36.
35. Kjell DP, Slattery BJ, Semo MJ. A novel nonaqueous method for regeneration of aldehydes from bisulfite adducts. J Org Chem 1999;64:5722–4.
36. Mishra A, Ma C-Q, Baüerle P. Functional oligothiophenes: molecular design for multidimensional nanoarchitectures and their applications. Chem Rev 2009;109:1141–276.
37. Tsai MS, Hsu YC, Lin JT, Chen HC, Hsu CP. Organic dyes containing 1*H*-phenanthro [9,10-*d*]imidazole conjugation for solar cells. J Phys Chem C 2007;111:18785–93.
38. Huang F, Chen KS, Yip HL, Hau SK, Acton O, Zhang Y, Luo JD, Jen AK-Y. Development of new cross-conjugated polymers with donor-π-bridge-acceptor side chains for high performance solar cells. J Am Chem Soc 2009;131:13886–7.
39. Williams ATR, Winfield SA, Miller JN. Relative fluorescence quantum yields using a computer-controlled luminescence spectrometer. Analyst 1983;108:1067–71.
40. Shortreed M, Kopelman R, Kuhn M, Hoyland B. fluorescent fiber-optic calcium sensor for physiological measurements. Anal Chem 1996;68:1414–8.
41. Lin W, Long L, Yuan L, Cao Z, Chen B, Tan W. A ratiometric fluorescent probe for cysteine and homocysteine displaying a large emission shift. Org Lett 2008;10:5577–80.
42. Lin Y, Lin W, Yang Y. A ratiometric fluorescent probe for specific detection of cysteine over homocysteine and glutathione based on the drastic distinction in the kinetic profiles. Chem Commun 2011;47:6275–7.
43. Kim TK, Lee DN, Kim HJ. Highly selective fluorescent sensor for homocysteine and cysteine. Tetra Lett 2008;49:4879–81.

Supporting information

Additional supporting information may be found in the online version of this article at the publisher's web site.